Journal of Science Research

2D Simulation of magnetotelluric data using finite element method

Joshua E.O.* and **Maduka M.**
Department of Physics, University of Ibadan, Nigeria
*Corresponding author: emmanuel.joshua@ui.edu.ng

Abstract

Finite element method to model plane-wave electromagnetic fields in 2D conductive structures has been developed. Triangular grids were used which readily conform to complicated geologic structures, unlike other existing numerical modeling techniques which are bound by the limitations of approximating complicated geologic structures using rectangular grids. Maxwell's equations were treated as a system of 2nd order partial differential equations and transformed into a weak form using method of weighted residuals. Application of this method for 2D Simulation of Magnetotelluric (MT) data, in transverse electric (E-polarization) mode, revealed that to obtain accurate results, a minimum thickness of the air layer is added to the model and is a function of the lateral conductivity contrasts within the earth. In the numeral model example, a minimum of 50 km air-layer thickness was added to nullify lateral changes in conductivity. Furthermore, Magnetotelluric (MT) transfer functions: impedance, apparent resistivity and impedance phase were also computed and their graphs displayed against the horizontal profile (y in km).

Keywords: Magnetotelluric modeling, electromagnetic theory, 2D simulation, finite element method, transfer functions

Introduction

The magnetotelluric method (MT) is an electromagnetic geophysical method used for inferring the electrical conductivity distribution of the earth's subsurface from the measurements of natural electric and magnetic fields on its surface. Electromagnetic techniques are widely used in mining exploration [1] and environmental applications [2] and are increasingly being used in hydrocarbon exploration [3]. The Earth's electromagnetic field generated contains a wide frequency spectrum. The low frequencies are generated by ionospheric and magnetospheric currents caused by solar wind interfering with the Earth's magnetic field. Higher frequencies, greater than 1Hz, are due to thunderstorms near equator distributed as guided waves between the Earth and the ionosphere [4]. Terminologically, when variations of frequencies lower than 10 Hz are used, we talk about Magnetotelluric (MT) method but for frequencies higher than 10 Hz we talk about Audio-frequency Magnetotelluric (AMT) method. The source resulting from low frequency variations penetrate, and hence probe, deep into the Earth but higher frequency variations probe shallow depths.

Numerical simulation of geo-electromagnetic field has been carried out for several decades and this keep developing due to the increasing need for reliability and accuracy of data acquisition techniques in numerical modelling [5-8]. Existing numerical modelling techniques commonly used are bound by the limitation of approximating complex structure [9] and were extensively reviewed in the papers [10,11]. Also, the difficulty in modeling electromagnetic field using Finite Element (FE) is possible jump of normal components across discontinuity of material properties and was resolved by curl-confirming elements of Nédélec [12]. The ability of Lagrange finite element to approximate the magnetotelluirc (MT) response of complex geological 2D structures have been demonstrated [13, 14].The issue of open, absorbing or non-reflecting boundary conditions that have to be implemented on a truncating boundary is one of the most intensively researched topics in the area of the numerical wave

propagation. These include the following popular techniques: variations of Bérenger's perfectly matched layers (PML) technique [15], the Dirichlet-to-Neumann (DEN) method [16] and the method of infinite elements [17]. In this paper, triangular grids finite-element (FE) approach was used, which readily conform to complicated structural boundaries, to obtained numerical solutions of a plane-wave time harmonic diffusive electromagnetic field (EM) in 2D conductivity structures.

Method

Electromagnetic field is generally described by the system of Maxwell's equations. In the case of quasi-stationary approximation of plane-wave, diffusive, time-harmonic electromagnetic fields in 2D conductivity structures, we neglected displacement current and introduced e^{jwt} in the Maxwell's equations to have the model equation as:

$$\nabla x\boldsymbol{E} = j\omega\mu\boldsymbol{H} \quad 1$$

$$\nabla x\boldsymbol{H} = \sigma\boldsymbol{E} \quad 2$$

Where $j^2 = -1$, angular frequency

$\omega = 2\pi f$, $\sigma = \sigma$

(y, z) = electric conductivity,

μ = magnetic permeability

Assuming a non-finite source and strike direction along x- axis of a 2D conductivity structure, equations 1 and 2 become

$$\frac{\partial Hz}{\partial y\partial z} - \partial Hy = \sigma E_x \quad 3a$$

$$\frac{\partial Ex}{\partial z} = j\omega\mu Hy \quad 3b$$

$$\frac{\partial Ex}{\partial y} = j\omega\mu Hz \quad 3c$$

and

$$\frac{\partial Ey - \partial Ez}{\partial z\partial y} = j\omega\mu H_x \quad 4a$$

$$\frac{\partial Hx}{\partial z} = \sigma E_y \quad 4b$$

$$\frac{\partial Hx}{\partial y} = \sigma E_z \quad 4c$$

for a homogeneous region of electrical conductivity, σ; where the occurrence of the electric field component E_x and the magnetic field components Hy and H_z in equations.3a – 3c is referred to as E – polarization, whereas equations.4a – 4c hold for the case of H – polarization.

Further combining equations.3a - 3c and 4a – 4c respectively yield two decoupled 2nd – order partial differential equations in terms of the strike aligned E_x and H_x fields.

For E – polarization:

$$\frac{\partial}{\partial y}\left(\frac{\partial E_x}{\partial y}\right) + \left(\frac{\partial\partial E_x}{\partial z\partial z}\right) - j\omega\sigma\mu E_x = 0 \quad 5a$$

For H – polarization

$$\frac{\partial\sigma-1}{\partial y}\frac{\partial Hx}{\partial y} + \frac{\partial\sigma-1}{\partial z}\frac{\partial Hx}{\partial z} - j\omega\mu H_x = 0 \quad 5b$$

in the bounded domain $\Omega \boldsymbol{\epsilon} R^2$

Boundary value problem

To solve equations 5a and 5b appropriate boundary conditions need to be introduced. Considering the simple model shown below (Figure 1).

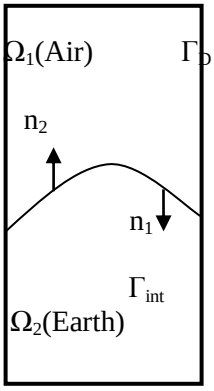

Figure1. Two arbitrary connected domains $\Omega_1$and$\Omega_2$with $\Omega = \Omega_1 \cup \Omega_2$, the outer Dirichlet boundary Γ_D, the inner boundary Γ_{int} and the outward unit normal vector n_1 and n_2 on Γ_{int}

The inner boundaries Γ_{int} representing jumps between regions of the piecewise constant model parameter σ, the tangential field components n x (o, H_y, H_z)^T and n x (o, E_y, E_z)^T are required to be continuous. Then, for the outer boundaries Γ_D, inhomogeneous Dirichlet boundary conditions are evaluated from 1D analytical solutions of a layered-earth model. This assumption is proven to be efficient when the modeling area boundary is far enough from the anomaly [18].

For E – polarization:

$$\frac{\partial}{\partial y}\left(\frac{\partial E_x}{\partial y}\right) + \left(\frac{\partial\partial E_x}{\partial z\partial z}\right) - j\omega\sigma\mu E_x = 0 \quad 6a$$

$$E_x = E_n\,(y, z) \text{ on } \Gamma_D \quad 6b$$

$$n_1 \text{ x } H_1 + n_2 \text{ x } H_2 = n_1 .(\nabla E_{x,1}) + n_2 . (\nabla E_{x,2}) = 0 \text{ on } \Gamma_{int} \quad 6c$$

and

For H – polarization

$$\frac{\partial\sigma-1}{\partial y}\frac{\partial Hx}{\partial y} + \frac{\partial\sigma-1}{\partial z}\frac{\partial Hx}{\partial z} - j\omega\mu H_x = 0 \quad 7a$$

$$H_x = H_n\,(y, z) \text{ on } \Gamma_D \quad 7b$$

$$n_1 \text{ x } E_1 + n_2 \text{ x } E_2 = n_1 .(\sigma^{-1}\nabla H_{x,1}) + n_2 . (\sigma^{-1}{}_2\nabla H_{x,2}) = 0 \text{ on } \Gamma_{int} \quad 7c$$

Hence, once the strike – parallel components E_x and H_x have been computed, the remaining components H_y, H_z, E_y and E_z can be derived from equations.3b, 3c, 4b and 4c by numerical differentiation in a subsequent procedure referred to as post-processing. Followed by the computation of the various MT transfer functions through the following equations;

For E – polarization:

Impedance, $Z_{TE} = \frac{E_x}{H_y}$ 8a

Apparent resistivity, $\rho_a = \frac{1}{\omega\mu}\left|\frac{E_x}{H_y}\right|^2$ 8b

Impedance phase $\Phi = \arctan\left[\frac{E_x}{H_y}\right]$ 8c

For H - polarization:

Impedance, $Z_{TM} = \frac{E_y}{H_x}$ 9a

Apparent resistivity, $\rho_a = \frac{1}{\omega\mu}\left|\frac{E_y}{H_x}\right|$ 9b

Impedance phase $\Phi = \arctan\left[\frac{E_y}{H_x}\right]$ 9c

Finite element approximation

The method of weighted residuals was used for the formulation of finite element approximations for the BVP by applying the vector identity (equation.11a), divergence theorem (equation.11b) and the Green's theorem (equations.11c,d) to the general form (equation.10) of equations.6a and7a:

- $\nabla . (a \nabla u) + bu = 0$ 10

Where

for E – polarization: $u = E_x$; $a = 1$, $b = j\omega\sigma\mu$

and in H – polarization: $u = H_x$; $a = \sigma^{-1}$; $b = j\omega\mu$

substituting into equation 10; we have

$a \nabla . b = \nabla = \nabla . (ab) - \nabla a.b$ 11a

$\int_\Omega \nabla.b \, d\Omega = \oint_\Gamma b.n d\Gamma$ 11b

$\int_\Omega \Phi \frac{\partial \psi}{\partial y} d\Omega = -\int_\Omega \psi \frac{\partial \psi}{\partial y} d\Omega + \oint_\Gamma \phi\psi \, n_y \, d\Gamma$ 11c

$\int_\Omega \Phi \frac{\partial \psi}{\partial z} d\Omega = -\int_\Omega \psi \frac{\partial \psi}{\partial z} d\Omega + \oint_\Gamma \phi\psi \, n_z \, d\Gamma$ [19] 11d

Resulting to discrete formulation

$(K + M) \vec{U} = 0$ 12

where K is the stiffness matrix and M is the mass matrix, for the vector $\vec{U}$ containing $N_{\Omega\backslash\Gamma D}$ elements of the interior points in region $\Omega\backslash\Gamma_D$ and $N_{\Gamma D}$ elements for the points on Γ_D whose values vanish.

Then, the inhomogeneous Dirichlet boundary condition is implemented for all interior points comprising $N_{\Omega}\backslash\Gamma_D$ zero-elements by assigning E_n values evaluated from 1D analytical solutions of a layered-earth model, in the case of E-polarization mode. The resulting linear equations are assembled and solved using MATLAB tool-box.

Numerical example

Calculations for BVP (equations 6a-c) were carried out using equations 10 and 8a-cand tested for robustness of our MATLAB code by considering a numerical model example for the E-polarization mode, which is shown in figure 2.

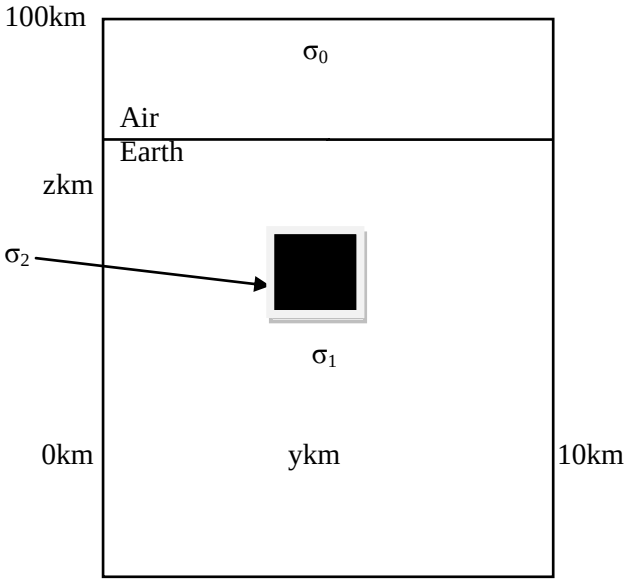

Figure 2. Numerical model example

The model consisted of a 100km by 10km thick slab with the air-layer inclusive. A square anomaly, which has a conductivity of $\sigma_2 = 0.5\ (\Omega m)^{-1}$ of dimension 2km by 2km, lays buried in an homogeneous background (the earth) with conductivity $\sigma_1 = 0.01\ (\Omega m)^{-1}$.

A grid size of 100 x 20 cells was used which yields 4000 triangular elements and frequency fixed at 1Hz.

Results and discussion

Influence of the air layer

Equatins.4b and 4c showed that the magnetic field component H_x is independent of the coordinates y and z within a non-conducting region. Hence, the air layer needed not to be introduced as part of our model. Unlike, the H-polarization models, the E-polarization models required the introduction of the air-layer as part of the model. This was as a result of the lateral in homogeneity in conductivity of the anomalous electric field which affects the real component of the electric field within the air-layer.

Thus, an air layer which is thick enough to reduce the secondary fields, produced by the lateral

in homogeneity in the earth to zero at the upper horizontal model boundary is required. For such air-thickness, the electric field at the top boundary is expected to be constant. Hence, the thickness of the air layer needs to be chosen with care in order to yield accurate results.

To this effect, we varied the air thicknesses to 10km, 20km and 50km and display the graphs of vertical profiles against the real component of the electric field.

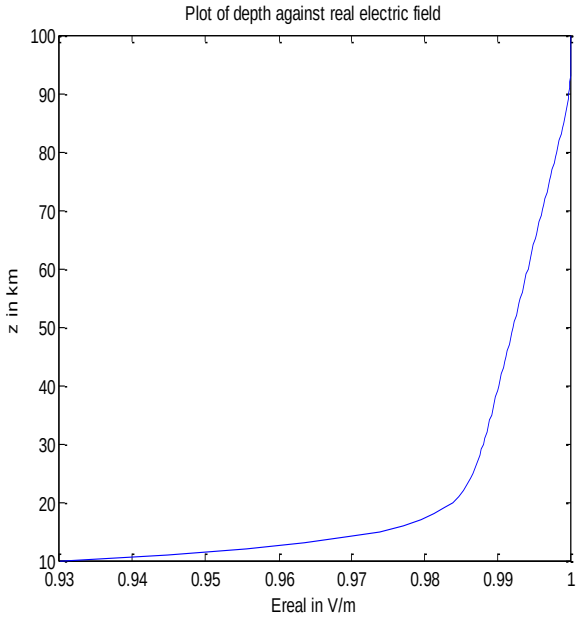

Figure 3. Plot of depth against real electric field (for 10km air thickness)

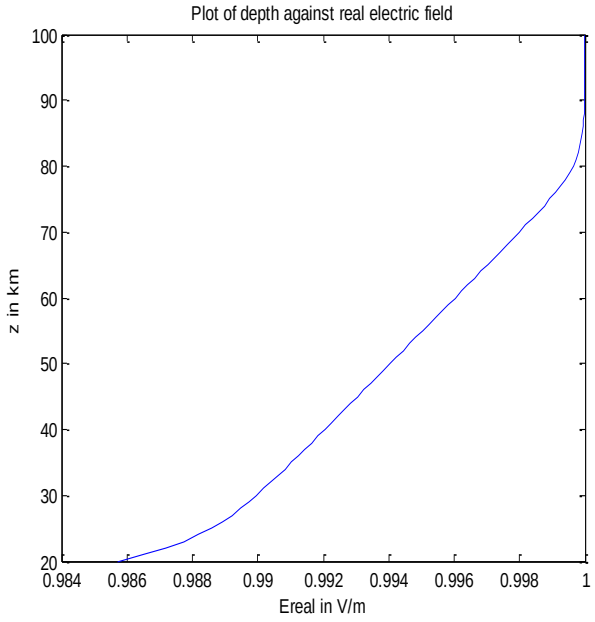

Figure 4. Plot of depth against real electric field (for 20km air thickness)

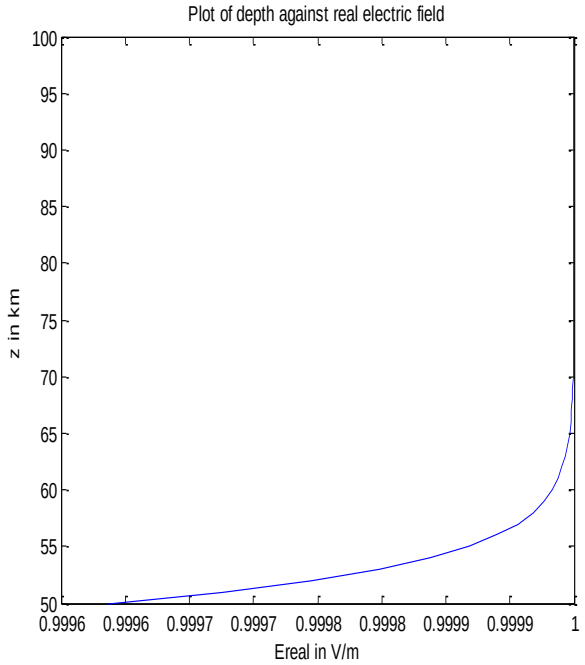

Figure 5. Plot of depth against real electric field (for 50km air thickness)

From our graphs, the anomalous field contributions along a vertical profile in the air layer obey a radiation contribution, hence, a reduction in the total field that converges asymptotically to the boundary value. Therefore, this behavior matches in the case of the 50km air layer, where the effect of the real part of the electric field E_x rose up to 70km. For air thicknesses 10km and 20km, it rose to 90km and almost linear where the thickness is 20 Km which is in contrast to a reduction in the total field E_x.

Transfer functions

It is common in MT simulations to display transfer functions because they are independent of the modulus of the impinging wave, usually unknown. With the air thickness at 50km,the graphs of the apparent resistivity and impedance phase against horizontal profile are as shown in figures 6 and 7 respectfully. The apparent resistivity decreases from 200 Ωm to 60 Ωm in the region of the buried object where it has its least resistivity values and then rises as it leaves the buried body.

This implies that the thickness of a reasonable air-thickness that will ensure that anomalous electric field vanishes at the top boundary is a function of the magnitude of the lateral conductivity contrasts. The same effect is seen from the impedance phase graph with the least phase shifts within the buried object region (figure 7).

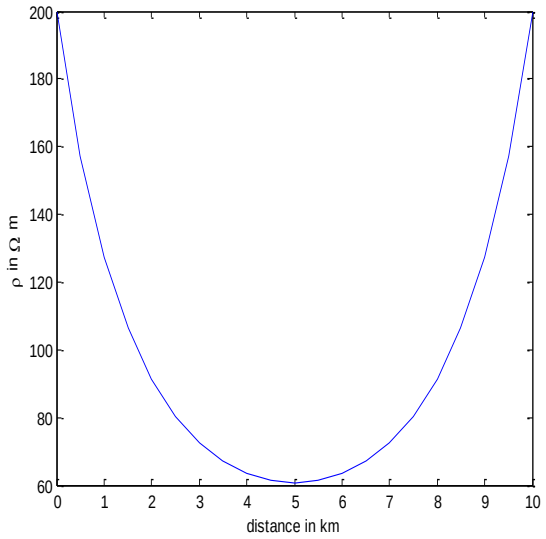

Figure 6. Plot of resistivity against horizontal profile

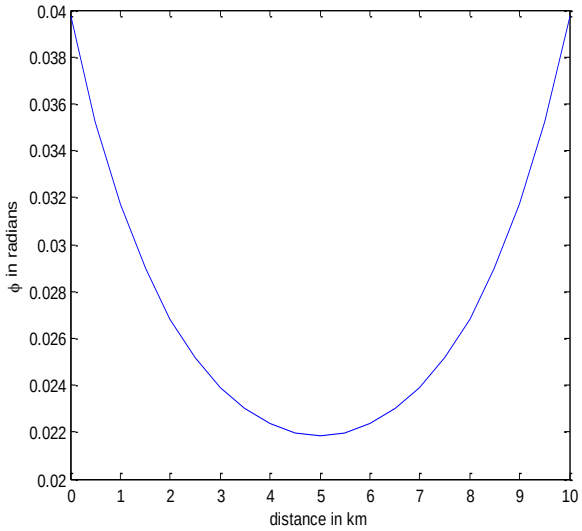

Figure7. Plot of Impedance phase against horizontal profile

Conclusion

We have presented a finite element algorithm using MATLAB to solve a 2D plane-wave diffusive time-harmonic electromagnetic fields with respect to magnetotelluric modeling.

The utilization of MATLAB's pde-toolbox has provided a unique tool for studying the response of complex 2D structures. Our numerical model has shown that our finite element approach is numerically robust. Our result showed that an air-thickness of 50km is sufficient to ensure this effect was well suited in the presence of anomalous structure in our model. This effect was also evident in the transfer functions displayed.

The next step to improving the accuracy and efficiency of our results in this project is to carry out adaptive refinement technique and effective convergence test. Comparisons of the results of this work with results obtained using other numerical approaches are also recommended.

Acknowledgements

We wish to acknowledge the support and technical guidance throughout this work of Prof. Colin Farquharson (Memorial University of Newfoundland, Canada) and Dr. E.O.Oyewande, Physics Department, University of Ibadan.

References

[1] Smith, R.(2014), Electromagetic Induction Methods in Mining Geophysics from2008-2012, *Surv. Geophys*.,35, 123-156.

[2] Reynolds, J.(2011), An introduction to applied and environmental geophysics, Wiley-Blackwell

[3] Strack, K.M.(2014), Future Directions of Electro-magnetic Methods for Hydro-carbon Applications, *Surv. Geophys*., 35, 157-177.

[4] Naidu, G.D. (2012). Deep crustal Structure of the Son-Narmada-Tapti Lineament, Central India, Springer Theses, DO I: 10.1007/978-3-642-28442-7_2

[5] Zyserman, F.I, Santos, J.E (2000). Parallel finite-element algorithm with domain decomposition of three-dimensional magnetotelluric modeling. *J. Appl Geophys* 44:337-351.

[6] Badea .E, Everett .M, Newman .G, Biro .O (2001). Finite element analysis of controlled-source electromagnetic induction using couloumb-gauged potentials. *Geophys* 66(3): 786-799.

[7] Pain .C, Herwanger .J, Worthington .M, Oliveira de C (2002). Effective multidimensional resistivity inversion using finite-element techniques. *Geophys J. Int*. 151(3): 710-728.

[8] Ruecker .C, Guenther .T, Spitzer .K (2006). Three-dimensional modeling and inversion of DC resistivity data incorporating topography. I. modeling.*Geophys J int* 166(2):495-505.

[9] Nedelec J.C (1980). Mixed finite-elements in R3. *Numer maths* 35:315-341.

[10] Avdeev D (2005) Three-dimensional electromagnetic modelling and inversion from Theory-toapplication. *SurvGeophys*.26:767–799.

[11] Ralph-Uwe Borner (2010). Numerical modeling in Geo-Electomagnetics: Advances and challenges. *Surv. Geophys* 31:225-245.

[12] Nedelec J.C (1986). A new family of mixed finite elements in R3. *Numer maths* 50:57-81.

[13] Key .K, and Weiss (2006). Adaptive finite-element modeling using unstructured grids: the 2D magnetotelluric example. *Geophys* 71(6): 185-200.

[14] Franke .A, Borner R.U., Spitzer .K (2007). Adaptive unstructured grid finite element stimulation of two-dimensional magnetotelluric fields for arbitrary surface and seafloor topography; *Geophays. J. Int*., 171 (1):71-86.

[15] Berenger J.P (1994). A perfect matched layer for the absorption of electromagnetic waves. *J. computer phys* 114(2): 185-200.

[16] Givoli .D (1999). Recent advances in the DtN FE Method. Arch comput methods Eng 6(2): 71-116.

[17] Demkowicz .L, Pal .M (1998). An infinite element for Maxwell's equations. Comput Method Appl Mech Eng. 164:77-94.

[18] Nam, M.J., Kim, H.J., Song, Y., Lee, T.J., Son, J.S., and Suh, J.H.(2007). 3D magnetotelluric modeling including surface topography: *Geophysical Prospecting*, **55**(2), 277 – 287.

[19] Zienkiewicz, O. C., 1977, The finite element method: McGraw-Hill Book Co.

Journal of Science Research ISSN 1119 7333
Citation: Joshua E.O. and Maduka M.
2D Simulation of magnetotelluric data using finite element method. Volume 16, 2017, pp 1-6